2013 IEEE/RSJ International Conference on
Intelligent Robots and Systems (IROS)
November 3-7, 2013. Tokyo, Japan

Steering Assist System for a Cycling Wheelchair based on Braking Control

Yasuhisa Hirata, Kazuhiro Kosuge, and Eric Monacelli

Abstract— **In this study, we propose a steering control method for a cycling wheelchair. The commercially available cycling wheelchair is a pedal-driven system that is similar to a bicycle, and patients with impairment of their lower extremities can move the wheelchair based on the pedaling force if they can slightly move their legs by themselves. The user can also change the wheelchair direction using the steering handle. However, right and left turns are perceived differently and a large steering torque is required while operating the steering handle because of hardware problems associated with the cycling wheelchair. To overcome this problem, we propose a new hardware solution and a method for steering motion control using servo brakes for the cycling wheelchair. The proposed method is applied to the developed cycling wheelchair, and the experimental results illustrate the validity of the system.**

Fig. 1. Commercially Available Cycling Wheelchair [3]

I. Introduction

Patients with severe impairment of the lower extremities use wheelchairs to improve their mobility. The patients typically use a manual wheelchair that is moved by applying a force to the wheel through the hand rim or an electric wheelchair operated by a joystick interface. In recent years, many researchers have proposed several types of intelligent wheelchairs that are controlled based on the human intention and environmental information [1], [2].

On the other hand, a new type of wheelchair named "Cycling Wheelchair" shown in Fig. 1 is currently available commercially [3]. The cycling wheelchair is a pedal-driven system that is similar to a bicycle, and wheelchair-bound patients with even slight leg mobility can easily rotate the pedal. Initially, Takazawa et al. proposed the cycling wheelchair at the Japanese symposium [4]. In [4], the disabled leg of the patients was moved by a functional electrical stimulation (FES) and the patients pedaled the cycling wheelchair based on the resulting motion of their legs. However, Takahashi et al. showed that hemiplegic patients can pedal the wheelchair without the application of an FES [5]. Results of many clinical tests have shown that not only hemiplegic patients but also many patients with severe impairment of the lower extremities, including paraplegic patients, can pedal the cycling wheelchair.

The cycling wheelchair was made available commercially by TESS Co. Ltd., Sendai, Japan [3], and is applied as not only a physical exercise machine in hospital rehabilitation, but also a mobility assist machine for improving the activity of daily living (ADL). Although patients are expected to use the cycling wheelchair in outdoor environments, there are several barriers such as steep slopes, steps, and obstacles. In our previous study, we developed a cycling wheelchair controlled by a regenerative brake system [6] and realized several assistive functions including velocity control, gravity compensation, and step/obstacle avoidance. In [6], we assumed that the cycling wheelchair performs 1 degree-of-freedom (DoF) motion and designed the assistive functions along a 1 DoF motion direction.

On the other hand, a steering assist system is also needed in the system, because the users perceive right and left turnings differently and a large steering torque is required while operating the steering handle. Although the users can change the wheelchair direction after training, its maneuverability should be improved to enable it to be used without training. In addition, it is difficult for caregivers to operate the commercially available cycling wheelchair because of the hardware problem associated with the steering control. Note that the reason for these problems will be explained in Section II.

To overcome the problems with the steering operation, we propose a new hardware for the cycling wheelchair and a steering motion control method that involves the use of servo brakes. If we can realize the steering control of the cycling wheelchair and if the wheelchair direction can be changed by using a hands-free interface such as body movement, the user can use both hands to do other tasks while operating the cycling wheelchair. This is a significant advantage of the cycling wheelchair compared to the conventional manual wheelchair operated by both arms in that it improves the activities that can be performed by the users.

In the following sections, we first consider the problems

Y. Hirata and K. Kosuge are with Department of Bioengineering and Robotics, Tohoku University, 6-6-01 Aoba, Aramaki, Aoba-ku, Sendai 980-8579, Japan. E. Monacelli is with LISV- Laboratoire d' Ingenierie des Systemes, Universite de Versailles Saint-Quentin-en-Yvelines, 10, 12 Avenue de l'Europe, 78140 Velizy, France. hirata@irs.mech.tohoku.ac.jp

978-1-4673-6357-0/13/$31.00 ©2013 European Union

with the steering system of the commercially available cycling wheelchair and introduce a new hardware for the cycling wheelchair with servo brakes. We then propose a braking control method for controlling the motion direction of the cycling wheelchair and experimentally evaluate the system.

II. Cycling Wheelchair with Brake System

First, we consider the hardware problem of the commercially available cycling wheelchair shown in Fig. 1. The cycling wheelchair is driven in a manner similar to a bicycle: the user applies torque by pedaling. The pedaling torque is transmitted only to the right wheel, and the left wheel is passive. A steering wheel is attached to the rear part of the wheelchair and is connected via a wire to an accessible steering handle.

Because the cycling wheelchair makes contact with the ground by three wheels, the wheelchair performs a 1 DoF rotational motion around an instantaneous center of rotation (ICR). The position of the ICR is determined by the angle of the steering wheel. Consequently, the user can control the wheelchair direction by operating the steering handle. The users perceive right and left turnings differently while operating the steering handle, because only the right wheel drives the wheelchair, and right turns are more difficult than left ones.

In addition to the operation requiring only the user, a caregiver can move the wheelchair from the rear to help the user in case of an insufficient driving force. In the case of a normal wheelchair, the caregiver can change the wheelchair direction by applying an intentional moment to the wheelchair without operation by the user. On the other hand, in the case of the cycling wheelchair, the user has to operate the steering handle to change the wheelchair direction, because the wheelchair direction is determined by the angle of the steering wheel. If the caregiver wants to transport the cycling wheelchair without a user, he/she has to lift up the steering wheel while turning the wheelchair.

To improve the maneuverability of the cycling wheelchair, in this study, we incorporate the structure of a normal wheelchair into a new cycling wheelchair. The normal wheelchair is supported by two wheels with hand rims and casters. Because the casters can passively move in all directions according to the direction of the applied force, the user can move the wheelchair easily by applying an arm force to each wheel through the hand rim. The caregiver can also operate the wheelchair direction based on intentional moment without operation by the user, because casters do not constrain wheelchair motion.

In this study, the steering wheel are removed from the cycling wheelchair, and casters are employed to stabilize its orientation, as with the normal wheelchair, to prevent falling accidents. Because the driving force of the cycling wheelchair is a large pedaling torque, it is difficult for the patients to apply arm forces to rotating wheels for steering operation. In addition, hemiplegic patients cannot operate both wheels using their arms.

To control the direction of motion of the cycling wheelchair without using the steering wheel, we attach servo brakes to the right and left wheels, as shown in Fig. 2. The output braking torque of a servo brake is transmitted to each wheel through a reduction gear and pulley. We also attach a differential gear between the pedal and the wheels, which distributes the pedaling torque equally to each wheel. By applying the braking torque to each wheel differently, the differential gear causes an angular velocity difference between the two wheels. As a result, the wheelchair changes the direction of motion. To specify the desired motion direction, we can design many types of interfaces such as a physical interface (e.g. a joystick), an interface using body postures, and a brain-machine interface. A hands-free interface enables the user to perform tasks that require both hands while operating the cycling wheelchair.

This study also focuses on the control of the servo brakes from a safety point of view. Goswami et al. [7] have proposed a safety-conscious concept named passive robotics and developed a Cobot architecture for a passive object handling system [8]. Other researchers have proposed dissipative haptic devices using brakes or clutches [9], [10]. We have also proposed several passive robot systems such as an object transporter [11], a walking assist system [12], and a haptic device [13], which are all controlled by servo brakes. These passive systems are intrinsically safe because they cannot move automatically under a driving force. In addition, regenerative brakes provide the steering control function with simultaneous charging of the battery [6]. Consequently, the system controlled by regenerative brakes would use little electricity and will require a small battery.

III. Steering Control using Servo Brakes

A. Desired Braking Force/Moment for Steering Control

To control the wheelchair direction, we determine the appropriate braking torque of each wheel. In this study, we propose a control method using a virtual steering wheel, as shown in Fig. 3. The virtual steering wheel can realize a steering operation feeling that is similar to that of the commercially available cycling wheelchair with a physical

Fig. 2. Developed Cycling Wheelchair

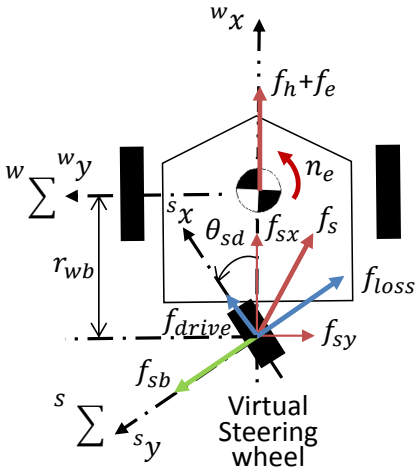

Fig. 3. Direction Control of Wheelchair with Virtual Steering Wheel

steering wheel when we specify the position of the virtual steering wheel relative to that of the physical steering wheel.

In addition, we can change the motion characteristic of the steering control by changing the position of the virtual steering wheel. If a user makes a large change to the steering angle when the linear velocity of the cycling wheelchair is high, a rapid rotational motion occurs. In this case, there is an increased risk of falling from the wheelchair. By setting r_{we}, which is the distance between the middle of the wheel axis and the virtual steering wheel, as shown in Fig. 3, to a large value, the straight motion is stabilized. On the other hand, when r_{wb} is small, the steering operation is sensitive. If we change the position of the virtual steering wheel relative to the front part of the cycling wheelchair, the steering feeling is similar to that of a car. Depending on one's disability and personal preferences, the steering characteristic can be adjusted.

Here, we define a wheelchair coordinate system ${}^{w}\Sigma$. The x-axis of the wheelchair coordinate system is the forward direction of the cycling wheelchair. We also define a virtual steering wheel coordinate system ${}^{s}\Sigma$. The x-axis of the virtual steering wheel coordinate system is the forward direction of the virtual steering wheel.

When the user pedals the cycling wheelchair, the human-applied force is applied to the origin of the wheelchair coordinate system as f_h. In addition, the disturbance force/moment f_e and n_e caused by the friction of the ground, force due to gravity on a slope, and so on are also applied to the origin of the wheelchair coordinate system. Note that the user cannot apply a moment to the wheelchair because the pedaling force is distributed equally to each wheel through the differential gear.

From f_h, f_e, and n_e, we calculate forces f_{sx} and f_{sy} that are applied to the origin of the virtual steering wheel coordinate system as follows:

$$f_{sx} = f_h + f_e \quad (1)$$

$$f_{sy} = \frac{n_e}{r_{wb}} \quad (2)$$

We divide the force applied to the steering wheel $f_s = [f_{sx},\ f_{sy}]^T$ into two forces: f_{drive} and f_{loss}. When the cycling wheelchair has a physical steering wheel, f_{loss} is compensated by the friction force between the physical steering wheel and the ground, and the rotational motion around the ICR, whose position is determined by the steering angle, is generated based on f_{drive}.

In this study, we apply a braking force f_{sb} to the origin of the virtual steering wheel, as shown in Fig. 3 to compensate for f_{loss}. That is, the braking force f_{sb} plays the role of the ground friction of the physical steering wheel. The braking force f_{sb} is calculated from $f_s = [f_{sx},\ f_{sy}]^T$ as follows:

$$f_{sb} = -(f_{sx}\sin\theta_{sd} + f_{sy}\cos\theta_{sd}) \quad (3)$$

where θ_{sd} is the desired angle of the virtual steering wheel. From f_{sb}, we calculate the desired braking force/moment $f_b,\ n_b$ applied to the middle of the wheel axis as follows:

$$f_b = f_{sb}\sin\theta_{sd} \quad (4)$$

$$n_b = r_{wb} f_{sb}\cos\theta_{sd} \quad (5)$$

Based on the desired braking force/moment, the cycling wheelchair without a steering wheel can change the direction of motion. However, we have to consider two issues. One is how to measure the human-applied force f_h and the disturbance force/moment $f_e,\ n_e$, which are used to calculate the desired braking force/moment. The other is the feasibility of the braking control because the output direction of the braking force is restricted according to the rotational direction of the wheel. We consider these two issues in the next subsection.

B. Estimation of Human-Applied Force and Disturbance Force/Moment

If the cycling wheelchair has a force sensor or a torque sensor attached to the pedal or the wheels, we can measure the human-applied force f_h. However, such sensors are generally expensive and fragile, and thus, impractical. In addition, we have to measure the disturbance force/moment $f_e,\ n_e$ caused by the friction force between the wheel and the ground, gravity on a slope, and so on. In this study, we estimate the force/moment including the human-applied force and the disturbance force/moment without using any special sensors.

Murakami et al. have proposed a disturbance observer for estimating the force/moment applied to the manipulator without using torque sensors [14] and developed a power assistive wheelchair [15] as one of the applications of the disturbance observer. We also proposed a power assistive bicycle and tricycle with a disturbance observer [16], which estimated the resistance forces applied to the cycle such as gravity force, window force, and friction force. In this study, we extend our proposed method [16] to the estimation of the force/moment including the human-applied force and the disturbance force/moment.

The dynamics of the wheelchair with respect to the middle of the wheel axis is expressed as

$$\boldsymbol{M}\ddot{\boldsymbol{X}} + \boldsymbol{D}\dot{\boldsymbol{X}} = \boldsymbol{F}_e - \boldsymbol{F}_b \quad (6)$$

where $\boldsymbol{M}$ denotes the inertial matrix of the cycling wheelchair and user, $\boldsymbol{D}$ denotes the damping matrix, and $\ddot{\boldsymbol{X}}$ and $\dot{\boldsymbol{X}}$ are the acceleration and velocity with respect to the x-axis of the wheelchair coordinate system and rotational direction around the origin of the wheelchair coordinate system, respectively. $\boldsymbol{F}_e = [f_h + f_e,\ n_e]^T$ is the force/moment applied to the cycling wheelchair by the human and environment, and $\boldsymbol{F}_b = [f_b,\ n_b]^T$ is the desired force/moment generated by the servo brakes.

From eq.(6), we can derive the state equation and the output equation as follows, assuming that the force/moment applied by the human and environment is constant.

$$\frac{d}{dt}\begin{bmatrix} \dot{\boldsymbol{X}} \\ \boldsymbol{F}_e \end{bmatrix} = \begin{bmatrix} -\frac{\boldsymbol{D}}{\boldsymbol{M}} & \frac{1}{\boldsymbol{M}} \\ 0 & 0 \end{bmatrix}\begin{bmatrix} \dot{\boldsymbol{X}} \\ \boldsymbol{F}_e \end{bmatrix} - \begin{bmatrix} \frac{\boldsymbol{F}_b}{\boldsymbol{M}} \\ 0 \end{bmatrix} \quad (7)$$

$$y = \begin{bmatrix} 1 & 0 \end{bmatrix}\begin{bmatrix} \dot{\boldsymbol{X}} \\ \boldsymbol{F}_e \end{bmatrix} \quad (8)$$

When we design a minimum order observer [16], the estimation force/moment $\hat{\boldsymbol{F}}_e$ is expressed as follows:

$$\hat{\boldsymbol{F}}_e = \frac{P}{s+P}(\boldsymbol{D}\dot{\boldsymbol{X}} - P\boldsymbol{M}\dot{\boldsymbol{X}} + \boldsymbol{F}_b) + P\boldsymbol{M}\dot{\boldsymbol{X}} \quad (9)$$

where P is the gain of the observer.

From the estimated force/moment $\hat{\boldsymbol{F}}_e$ and eqs.(1)-(5), we can calculate the desired braking force/moment required to realize the steering control. However, we cannot accurately estimate the human force and disturbance force/moment if the inertial matrix $\boldsymbol{M}$ and damping matrix $\boldsymbol{D}$, which are used for the estimation of the force/moment, are not determined. Particularly, in the case of the cycling wheelchair, many persons with different weights use the cycling wheelchair, and the friction between the wheels and the ground changes with the environmental conditions.

To overcome this problem, we add a feedback term to control the rotational motion of the cycling wheelchair. When the disturbance observer cannot estimate the force/moment accurately, the brake system cannot compensate for the f_{loss} applied to the virtual steering wheel and an uncompensated force is applied to the perpendicular direction of the forward direction of the virtual steering wheel. As a result, the cycling wheelchair moves according to the resultant force of the driving force f_{drive} and the uncompensated force. This means the desired and actual angles of the virtual steering wheel do not match. Therefore, we recalculate the desired braking moment with the difference between the desired and actual angles of the steering wheel as the feedback term.

The actual angle of the steering wheel θ_s is determined by the actual motion of the cycling wheelchair as follows:

$$\theta_s = \tan^{-1}(\frac{r_{wb}\dot{\theta}}{\dot{x}}) \quad (10)$$

where $\dot{x}$ and $\dot{\theta}$ are the velocity and angular velocity of the cycling wheelchair, respectively. Under the assumption that the desired angle of the cycling wheelchair θ_{sd} is given by a simple interface such as a joystick or by environmental information, the desired braking moment expressed in eq. (5) is rewritten as follows:

$$n_b = -r_{wb}f_{sb}\cos\theta_{sd} + k_s(\theta_{sd} - \theta_s) \quad (11)$$

where k_s is the feedback gain.

C. Control based on Feasible Braking Control Region

In braking control, we have to consider a feasible braking control region calculated by the brake control limitation. This means that the servo brake merely prevents the rotational motion of the wheel. Therefore, the following relationship exists between the angular velocity of the wheel and the braking torque of the wheel.

$$\tau_b\omega \leq 0 \quad (12)$$

where τ_b denotes the braking torque and ω denotes the angular velocity of the wheel. In our previous studies, we used the powder brake and the magnetic rheological (MR) brake to control passive robots [11], [12], [13]. In this study, we use a DC servo motor as a servo brake because it has high responding compared to the powder and MR brakes, and we are interested in its use as a regenerative brake system in the future. Unlike the brake condition of the powder and MR brakes, the DC servo motor cannot generate the braking torque when its angular velocity is equal to zero [6]. Therefore, we define the maximum braking torque $\tau_{b_{max}}$ as an additional braking condition according to the angular velocity of the wheel ω as follows:

$$\tau_{b_{max}} = -d\omega \quad (13)$$

where $d > 0$. Note that the initial torque caused by the mechanical friction of the servo brake increases the pedaling torque of the human even if we do not control the serve brake. However, the initial torque of the DC servo motor is small, and we have confirmed that the user does not feel the load from the initial torque when operating without braking control.

The DC servo motor attached to the cycling wheelchair has an encoder that allows us to calculate the angular velocity of each wheel. The feasible braking control region is derived from the brake condition determined by the angular velocity of each wheel. In the wheelchair coordinate system, the wheelchair velocity is expressed as $\dot{\boldsymbol{X}} = [\dot{x},\ \dot{\theta}]^T$, where x and θ denote the linear and rotational components of the motion, respectively. The angular velocities of the right and left wheels are $\boldsymbol{\omega} = [\omega_r,\ \omega_l]^T$. The wheelchair velocity is related to the wheel motions through the following equation by using the Jacobian $\boldsymbol{J}$:

$$\dot{\boldsymbol{X}} = \boldsymbol{J}\boldsymbol{\omega}\ . \quad (14)$$

The relationship between the braking torque of each wheel $\boldsymbol{\tau}_b = [\tau_{br},\ \tau_{bl}]^T$ and the force/moment applied to the wheelchair $\boldsymbol{F}_b = [f_b,\ n_b]^T$ in the wheelchair coordinate system is

$$\boldsymbol{\tau}_b = \boldsymbol{J}^T\ \boldsymbol{F}_b\ . \quad (15)$$

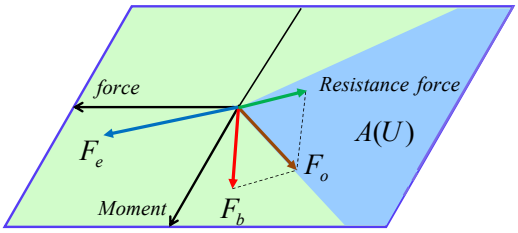

Fig. 4. Brake Control based on Feasible Braking Control Region

The set of feasible braking torques of each wheel $U(\boldsymbol{\omega})$ is expressed in terms of the brake control condition of eq.(12) and eq.(13) as follows:

$$U(\boldsymbol{\omega}) = \{\tau_{br}\mathbf{e}_1 + \tau_{bl}\mathbf{e}_2 \mid \tau_{br}\omega_r \leq 0,\ \tau_{bl}\omega_l \leq 0, \ |\tau_{br}| \leq \tau_{br_{max}},\ |\tau_{bl}| \leq \tau_{bl_{max}}\} \tag{16}$$

where

$$\begin{bmatrix} \mathbf{e}_1 & \mathbf{e}_2 \end{bmatrix} = diag(1,1)\ . \tag{17}$$

The feasible braking control region $A(U)$, derived from $U(\boldsymbol{\omega})$, is expressed as

$$A(U) = \{\tau_{br}\mathbf{v}_1 + \tau_{bl}\mathbf{v}_2 \mid \tau_{br},\ \tau_{bl} \in U(\boldsymbol{\omega})\ \} \tag{18}$$

where

$$\begin{bmatrix} \mathbf{v}_1 & \mathbf{v}_2 \end{bmatrix} = \boldsymbol{J}^T \begin{bmatrix} \mathbf{e}_1 & \mathbf{e}_2 \end{bmatrix}\ . \tag{19}$$

The desired force/moment is directly generated by the DC servo motor only when specified within the feasible braking control region. Otherwise, the situation shown in Fig. 4 arises. In most cases involving steering control, the desired braking moment is outside the feasible braking control region. For example, when we want to turn right, the desired braking moment is negative. When we derive the braking torque of each wheel simply by using eq.(11), the left wheel has to be accelerated, but the brake system cannot accelerate the wheel.

If the desired force/moment is outside the feasible braking control region, as shown in Fig. 4, a wheel that can output an adequate braking torque has to generate a large braking torque to realize the braking moment shown in eq.(11). We determine the output braking force applied to each wheel, denoted as $F_o = [f_{or},\ f_{ol}]^T$. When the wheelchair turns left, the angular velocity of the left wheel is decreased. Consequently, the left wheel cannot generate a large braking force. To realize the desired moment, the left wheel compensates for this loss as follows:

$$f_{or} = \frac{n_b - f_{ol}(-T/2)}{T/2} \tag{20}$$

where T is the distance between the right and left wheels. On the other hand, when the wheelchair turns right, we have

$$f_{ol} = \frac{n_b - f_{or}(-T/2)}{T/2}\ . \tag{21}$$

The above equations yield multiple solutions of f_{or} and f_{ol} in the feasible braking control region. We now consider how to determine the output braking force/moment. The braking force/moment determined by these equations can be divided into two elements: the desired moment and the resistance force compensated by the user along the forward direction. When the driving force applied by the user exceeds the resistance force, the cycling wheelchair moves forward and also realizes the desired motion. However, if the resistance force is large, the burden on the user increases. In this study, to maximally reduce the burden on the user, the braking force/moment is determined at the boundary of the feasible braking control region, as shown in Fig. 4.

IV. Experiments for Steering Control

The proposed method was applied to the developed cycling wheelchair to experimentally confirm its validity. First, we specified the desired angle of the virtual steering wheel using a simple interface. By operating the interface, the user changed the motion direction intentionally. Next, we assumed that the desired angle of the virtual steering wheel was calculated according to the environment information, and then we conducted a path following experiment and an obstacle avoidance experiment. A healthy subject conducted the experiments. The gains of the control method were experimentally determined. The experimental results are shown in the following sections and the accompanying video.

A. Steering Control using Manual Interface

In this experiment, we attached a potentiometer to the cycling wheelchair as an interface for steering control. Using the potentiometer, the subject performed the following operations in the given sequence: turn right, move straight, turn left, move straight, turn left, and move straight. Experimental results are shown in Fig. 5. Fig. 5(a) shows the desired and actual angles of the virtual steering wheel, and Fig. 5(b) shows the path of the cycling wheelchair. Because the inertial moment of the potentiometer was very small, the desired angle of the virtual steering wheel was almost a step input. In the steady state, the actual angle of the virtual steering wheel converged to the desired angle and the subject could move the cycling wheelchair intentionally.

In Fig. 6, we show examples of the feasible braking control region, desired braking force/moment, and output braking force/moment during the experiment. In Fig. 6(a), the desired force/moment was outside the feasible braking control region. However, the desired moment was appropriately generated to realize the steering control. In Fig. 6(b), the brake system could not generate a sufficient braking moment to control the steering motion because the desired virtual steering angle is changed significantly and rapidly. As a result, the maximum braking force/moment was generated. In these cases, the burden on the user increased because the user had to apply the driving force through the pedal to generate the desired moment. However, the subject did not feel a large burden during the experiment. We will quantitatively evaluate the burden on the user in a future study. On the other hand, in

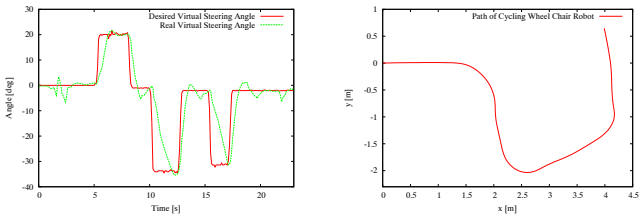

(a) Angle of Steering Wheel (b) Path of Cycling Wheel Chair

Fig. 5. Experimental Results of Manual Steering Control

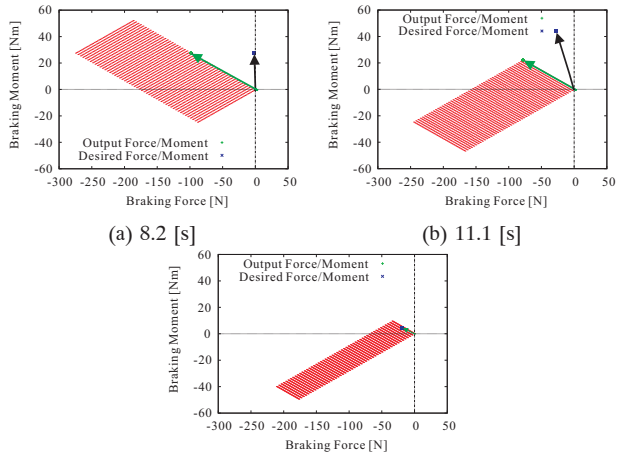

(a) 8.2 [s] (b) 11.1 [s]

(c) 12.2 [s]

Fig. 6. Feasible Braking Control Region

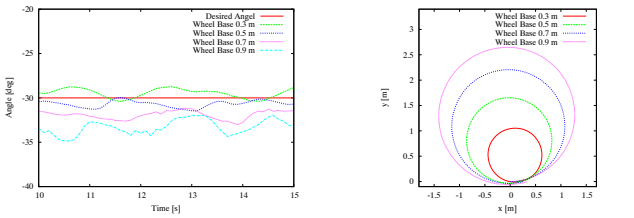

(a) Angle of Steering Wheel (b) Path of Cycling Wheelchair

Fig. 7. Experiments by Variable Rotational Characteristic Control

Fig. 6(c), the desired braking force/moment was within the feasible braking control region. Therefore, the output braking force/moment coincided with the desired force/moment.

Next, we changed the steering characteristic of the wheelchair by changing the position of the virtual steering wheel. In this experiment, we rotated the cycling wheelchair with four positions of the virtual steering wheel. In the experiments, r_{wb} was specified as 0.3 [m], 0.5 [m], 0.7 [m], and 0.9 [m]. We also specified the desired angle of the virtual steering wheel as -30 [deg] in all experiments. Actual angles of the virtual steering wheel were almost -30 [deg], as shown in Fig. 7(a). On the other hand, the paths of the cycling wheelchair were changed in these experiments, as shown in Fig. 7(b). These results show that the steering characteristic can be changed according to the position of the virtual steering wheel.

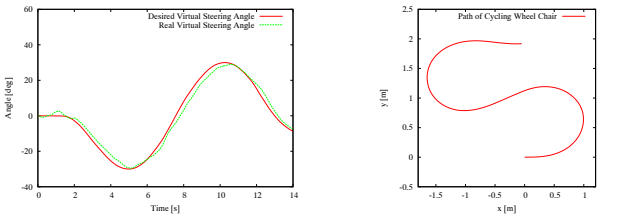

(a) Angle of Steering Wheel (b) Path of Cycling Wheelchair

Fig. 8. Experimental Results of Path Following Control

B. Path Following and Obstacle Avoidance Experiments

We performed a path following experiment by specifying the desired angle of the virtual steering wheel. We determined the desired angle using the equation $\theta_{sd} = 30 \sin x$ [deg], where x is the moving distance of the cycling wheelchair with respect to the forward direction. Using this equation, the cycling wheelchair moves along an S-shaped path. By equipping the wheelchair with a sensor to detect a line on the ground, we can calculate the desired angle of the virtual steering wheel from its ground information. Fig. 8(a) shows the actual and desired angles of the virtual steering wheel and Fig. 8(b) shows the actual path of the cycling wheelchair. These results show that the cycling wheelchair moves along the desired path.

In addition to the path following experiment, we conducted an obstacle/step avoidance experiment. In this experiment, we assumed the presence of an obstacle ahead of the wheelchair because the obstacle/step detection sensor was not yet attached to the wheelchair. Although robotics researchers have proposed many methods for avoiding obstacles/steps, we designed a simple method for only illustrating the obstacle/step avoidance function of the cycling wheelchair, as shown in Fig. 9.

We designed a repulsive force f_o with respect to the perpendicular direction of the moving direction of the cycling wheelchair as follows:

$$f_o = -\frac{k_o}{r_{oy}} \tag{22}$$

where k_o is positive constant and r_{oy} is the distance between the obstacle and a point P, as shown in Fig. 9. This equation means that the repulsive force increases when r_{oy} is small. From f_o and r_{ox}, we define the desired angle of the virtual steering wheel θ_{so} for obstacle avoidance as follows:

$$\theta_{so} = -\tan^{-1}\frac{f_o}{r_{ox}} \ . \tag{23}$$

If the desired angle given by the manual interface is defined as θ_{sm}, the desired angle of the virtual steering wheel θ_{sd} is changed as follows:

$$\theta_{sd} = \alpha\theta_{sm} + (1-\alpha)\theta_{so} \tag{24}$$

where α is a weighting factor ($0 \leq \alpha \leq 1$). When there is an obstacle around the cycling wheelchair, we specify α with a small value. In this case, the obstacle avoidance function has high priority. When α has a large value in a free environment,

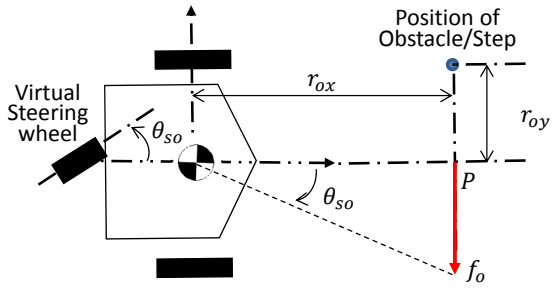

Fig. 9. Obstacle/Step Avoidance Control

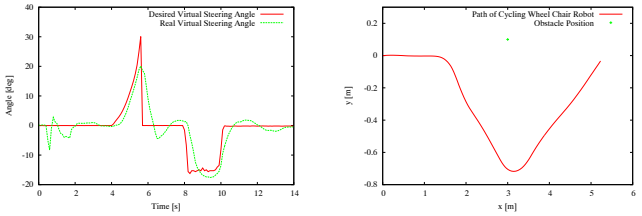

(a) Angle of Steering Wheel (b) Path of Cycling Wheel Chair

Fig. 10. Experimental Results for Obstacle Avoidance

the user can operate the cycling wheelchair based on manual control using the interface as explained in section IV-A.

In this experiment, we assumed that $r_{ox} = 3.0$ [m] and $r_{oy} = 0.1$ [m] with respect to the initial wheelchair position, and the initial angle of the virtual steering wheel was 0 [deg]. We also used $\alpha = 0.5 r_{ox}$ to realize obstacle avoidance functions when r_{ox} is less than 2 [m]. While approaching the obstacle, the subject did not operate the interface (potentiometer). After passing the obstacle, the subject controlled the motion direction using the interface. The experimental result is shown in Fig. 10. Fig. 10(a) shows the desired and actual angles of the virtual steering wheel, and Fig. 10(b) shows the path of the cycling wheelchair. When r_{ox} was less than 2 [m] after 3 [s], the desired and actual angles of the virtual steering wheel were changed to avoid the obstacle. After passing the obstacle, the steering angles returned to 0 [deg], and the subject then operated the steering angle manually for turning left. From this result, we observe that the obstacle avoidance function is realized appropriately. In future studies, we will use the obstacle/step avoidance methods proposed thus far to specify the desired angle of the virtual steering wheel in complicated environments.

V. Conclusions and Future Works

In this study, we developed a new cycling wheelchair with differential gear and servo brakes, and proposed a steering control method based on the feasible braking control region. With this method, the wheelchair direction can be changed by specifying the desired angle of the virtual steering wheel. The obtained experimental results illustrated the validity of the proposed method.

Therapists and medical doctors have evaluated the cycling wheelchair. They rated the steering control using a simpler interface such as a joystick very highly, and it is expected to realize a hands-free operation. If a subject can command the direction of the cycling wheelchair by using his/her body movements, the wheelchair can be controlled without the use of hands. The hands-free operation would improve the ADL of users. We will evaluate the validity of the proposed cycling wheelchair by performing extensive testing on disabled patients, therapists, and medical doctors, and on the basis of their feedback, we will subsequently improve the hardware and control method.

Acknowledgments

We would like to thank Prof. Yasunobu Handa of Tohoku University for providing several medical datasets, Mr. Kenji Suzuki of TESS Co. Ltd. for providing a prototype of the cycling wheelchair, and the CEREMH (Center de Ressources & d'lnnovation Mobilite Handicap) for providing the opportunity for therapists to evaluate the proposed cycling wheelchair.

References

[1] D. P. Miller, M. G. Slack, "Design and Testing of a Low-cost Robotic Wheelchair Prototype", *Autonomous Robotics*, Vol. 2, pp. 77-88, 1995.

[2] L. M. Bergasa, M. Mazo, A. Gradel, M. A. Sotelo, J. C. Garcia, "Guidance of a Wheelchair for Handicapped People by Head Movements", *Proceedings of International Conference on Field and Service Robotics*, pp. 150-155, 1999.

[3] http://www.h-tess.com/ (March 15, 2013)

[4] M. Takazawa, M. Shoji, T. Takahashi, E. Nakano, Y. Handa, "A Power-assisted FES Cycling Wheel Chair for the Lower Limbs Disabled", *Proceedings of JSME Symposium on Welfare Engineering*, pp. 209-212, 2002 (in Japanese).

[5] T. Takahashi, K. Seki, "A Novel Leg-Driven Wheelchair for Person with Lower Limbs Paralysis", *Journal of the Society of Instrument and Control Engineers*, Vol. 45, No. 5, pp. 440-444, 2006 (in Japanese).

[6] Y. Hirata, K. Kawamata, K. Sasaki, A. Kaisumi, K. Kosuge, E. Monacelli, "Regenerative Brake Control of Cycling Wheelchair with Passive Behavior", *Proceedings of IEEE International Conference on Robotics and Automation*, pp. 3858-3864, 2013.

[7] A. Goswami, M. A. Peshkin, J. Colgate, "Passive robotics: an exploration of mechanical computation (invited)", *Proceedings of the IEEE International Conference on Robotics and Automation*, pp. 279-284, 1990.

[8] M. A. Peshkin, J. E. Colgate, W. Wannasuphoprasit, C. A. Moore, R. B. Gillespie, P. Akella, "Cobot Architecture", *IEEE Transactions on Robotics and Automation*, Vol. 17, No. 4, 2001.

[9] D. Gao, W. J. Book, "Steerability in Planar Dissipative Passive Robots", *The International Journal of Robotics Research*, Vol. 29, No. 4, pp. 353-366, 2010.

[10] B. Dellon, Y. Matsuoka, "Path Guidance Control for a Safer Large Scale Dissipative Haptic Display", *Proc. of the IEEE International Conference on Robotics and Automation*, pp. 2073-2078, 2008.

[11] Y. Hirata, Z. Wang, K. Fukaya, K. Kosuge, "Transporting an Object by a Passive Mobile Robot with Servo Brakes in Cooperation with a Human", *Advanced Robotics*, Vol. 23, No. 4, pp. 387-404, 2009.

[12] Y. Hirata, A. Hara, K. Kosuge, "Motion Control of Passive Intelligent Walker Using Servo Brakes", *IEEE Transactions on Robotics*, Vol. 23, No. 5, pp. 981-990, 2007.

[13] Y. Hirata, K. Suzuki, K. Kosuge, "Motion Control of Passive Haptic Device Using Wires with Servo Brakes", *Proceedings of the 2010 IEEE/RSJ International Conference on Intelligent Robots and Systems*, pp. 3123-3129, 2010.

[14] T. Murakami, F. Yu, K. Ohnishi, "Torque Sensorless Control in Multidegree-of-Freedom Manipulator", *IEEE Transaction on Industrial Electronics*, Vol. 40, No. 2, pp. 259-265, 1993.

[15] S. Tashiro, T. Murakami, "Power-Assist Control of an Electric Wheelchair Considering Step Passage", *Proceedings of 2007 IEEE/ASME International Conference on Advanced Intelligent Mechatronics*, pp. 1-6, 2007.

[16] H. Yabushita, Y. Hirata, K. Kosuge, Z. Wang, "Environment-Adaptive Control Algorithm of Power Assisted Cycle", *Proceedings of the IECON*, pp. 1962-1968, 2003.